

Chiral phase transition and Anderson localization in the Instanton Liquid Model for QCD

Antonio M. García-García

*Physics Department, Princeton University, Princeton, New Jersey 08544, USA and
The Abdus Salam International Centre for Theoretical Physics, P.O.B. 586, 34100 Trieste, Italy*

James C. Osborn

Physics Department & Center for Computational Science, Boston University, Boston, MA 02215, USA

We study the spectrum and eigenmodes of the QCD Dirac operator in a gauge background given by an Instanton Liquid Model (ILM) at temperatures around the chiral phase transition. Generically we find the Dirac eigenvectors become more localized as the temperature is increased. At the chiral phase transition, both the low lying eigenmodes and the spectrum of the QCD Dirac operator undergo a transition to localization similar to the one observed in a disordered conductor. This suggests that Anderson localization is the fundamental mechanism driving the chiral phase transition. We also find an additional temperature dependent mobility edge (separating delocalized from localized eigenstates) in the bulk of the spectrum which moves toward lower eigenvalues as the temperature is increased. In both regions, the origin and the bulk, the transition to localization exhibits features of a 3D Anderson transition including multifractal eigenstates and spectral properties that are well described by critical statistics. Similar results are obtained in both the quenched and the unquenched case though the critical temperature in the unquenched case is lower. Finally we argue that our findings are not in principle restricted to the ILM approximation and may also be found in lattice simulations.

PACS numbers: 72.15.Rn, 71.30.+h, 05.45.Df, 05.40.-a

I. INTRODUCTION

By now it is well established that many of the properties of light hadrons are dictated by spontaneous chiral symmetry breaking ($S\chi SB$) due to the nonperturbative structure of the QCD vacuum. However, in the high temperature limit, non perturbative effects are suppressed and chiral symmetry is eventually restored at a certain critical temperature. Recent lattice simulations suggest furthermore that both the restoration of chiral symmetry and the confinement-deconfinement transition occur at the same temperature [1]. A detailed account of the microscopic mechanisms leading to $S\chi SB$ and confinement and the eventual restoration and deconfinement remains among the most formidable challenges in hadronic physics. In recent years the combination of experimental results and novel lattice techniques have greatly clarified the nature and properties of these transitions. However we are still far from a full microscopic understanding of the chiral phase transition and its relation to the confinement-deconfinement transition. In this paper we examine how the phenomenon of Anderson localization [2], originally introduced in the field of condensed matter physics, may help to understand the mechanism driving the chiral phase transition. Specifically, in the context of an Instanton Liquid Model (ILM), we show that near the temperature around which the chiral phase transition occurs the low lying eigenmodes of the QCD Dirac operator undergo a localization-delocalization transition consistent with an Anderson transition (AT) characterized by multifractal eigenstates and critical statistics [2]. In order to make accessible our findings to a broader audience, we first provide short summaries on the role of instantons in the non-perturbative structure of QCD, similarities between the QCD vacuum and a disordered medium, the QCD chiral phase transition and finally a brief overview on the properties of a disordered conductor at an AT. In section II we will present our results for the ILM simulations in both the quenched case and the unquenched case for two and three flavors. In section III we discuss the relationship of our results with current lattice simulations followed by conclusions in section IV.

A. Instanton Liquid Models and $S\chi SB$

Instantons [3] are classical solutions of the Yang-Mills equations of motion which minimize the action in Euclidean space. They are believed to be the leading semiclassical contribution to the bosonic part of the QCD path integral. However the construction of a consistent QCD vacuum based on instantons faces serious technical difficulties. Exact multi-instanton solutions are hard to obtain since the Yang-Mills equations of motion for QCD are nonlinear and therefore a superposition of single instanton contributions is not itself a solution. Additionally quantum corrections may spoil the semiclassical picture implicitly assumed of a QCD vacuum composed of instantons well separated

and weakly interacting. These problems have been overcome either by invoking variational principles [4] or by phenomenologically fixing certain parameters of the instanton ensemble. The latter case, usually referred to as the instanton liquid model (ILM) [5] (for a modern review see [6]), yields accurate estimates of vacuum condensates and hadronic correlation functions [7] for most light hadrons just by setting the mean distance between instantons to be $\bar{R} \approx 1$ fm (which corresponds to a density $N/V \sim 1 \text{ fm}^{-4}$) and the mean instanton size $\bar{\rho} \approx 1/3$ fm. Lattice simulations have also supported the picture of a QCD vacuum dominated by instantons [8].

One of the main success of the ILM is its convincing explanation of how chiral symmetry is spontaneously broken in the QCD vacuum [4, 5]. The starting point is the fact that the Euclidean QCD Dirac operator has an exact zero eigenvalue in the field of an instanton. In an ensemble of (anti-)instantons the overlap of neighboring instantons makes the would-be zero modes effectively split around zero. In the limit of large number of (anti-)instantons a continuous band spectrum is formed with a spectral density finite at zero. The spectral properties of the low lying modes of the Dirac operator are thus controlled by these non-perturbative configurations. It turns out that the order parameter associated with spontaneous chiral symmetry breaking $\langle \bar{\psi}\psi \rangle$ (the chiral condensate) is indeed related to the spectral density $\rho(\epsilon)$ of the QCD Dirac operator around zero through the Banks-Casher relation [9],

$$\langle \bar{\psi}\psi \rangle = - \lim_{\epsilon \rightarrow 0} \lim_{V \rightarrow \infty} \frac{\pi \rho(\epsilon)}{V}, \quad (1)$$

where V is the space-time volume. We are therefore interested in modeling the lowest eigenvalues of the Dirac operator. The ILM provides a phenomenological model for these low energy modes of the QCD Dirac operator. In a basis of $N/2$ instantonic zero modes $\psi_I^{(i)}$ and $N/2$ anti-instantonic zero modes $\psi_A^{(j)}$ the matrix elements of the Dirac operator take the form (for zero quark mass)

$$\mathcal{D}_{ILM} = \begin{pmatrix} 0 & iT_{IA} \\ iT_{IA}^\dagger & 0 \end{pmatrix}. \quad (2)$$

In the limit of large separations $\vec{R}_{ij} = \vec{z}_i - \vec{z}_j$ between the center of instanton i and anti-instanton j the elements of the $N/2 \times N/2$ overlap matrix T_{IA} decay as a power-law,

$$[T_{IA}]_{i,j} = \langle \psi_I^{(i)} | \not{D} | \psi_A^{(j)} \rangle \sim \rho_i \rho_j / |\vec{R}_{ij}|^3 \quad (3)$$

with ρ_i and ρ_j their respective sizes and \not{D} is the Dirac operator. Many properties of the QCD vacuum can then be estimated from the matrix elements of T_{IA} . For example the chiral condensate can be calculated as $\langle \bar{\psi}\psi \rangle \approx -(215 \text{ MeV})^3$ [4, 6] which is reasonably close to the experimental value.

B. The QCD vacuum as a disordered medium

In recent years it has been suggested [10, 11, 12, 13] that the $S\chi SB$ in QCD and the phenomenon of conductivity in a disordered medium have similar physical origins. Conductivity in a disordered sample is produced by electrons that although initially bound to an impurity may get delocalized by orbital overlapping with nearby impurities. Similarly, in the QCD vacuum, the zero modes of the Dirac operator though initially bound to an instanton may get delocalized due to the strong overlap with other instantons. As a consequence, the chiral condensate becomes nonzero and chiral symmetry is broken.

In the case of electrons the overlap is effective only among nearest neighbors since the electron wavefunction has an exponential tail. On the contrary, in the QCD vacuum, quark zero modes can travel long distances in the QCD vacuum. Hopping is not restricted to nearest neighbors since the probability for a quark to hop between an instanton and an anti-instanton has a power-law tail in the pseudo-particle distance (equation 3). As we discuss next, eigenvectors of quantum systems with this kind of long range hopping are delocalized in four (and higher) dimensions [14, 15].

Localization properties of a disordered system are strongly influenced by factors such as the dimensionality of the space, the strength of disorder and the hopping range. For short range hopping it is well known that, in three and higher dimensions and for a certain range of impurity amount, a system will have a mobility edge separating localized from a delocalized eigenstates. Eigenstates around the mobility edge (the Anderson transition region) are multifractal and the level statistics (commonly referred to as *critical statistics* [16]) are universal and intermediate between Wigner-Dyson (WD) and Poisson statistics (for a review see [17]).

An Anderson transition is also observed in disordered systems with power-law hopping [14, 15, 18] provided that the exponent of the hopping decay matches the dimension of the space. If the exponent is larger (smaller) than the dimension of the space then the eigenstates becomes localized (delocalized). In this case the localization properties in the thermodynamic limit depend only on the power-law decay and not on the strength of disorder. Since in QCD

at zero temperature the dimensionality of the space (four) is larger than the hopping decay power (three, see equation 3), one expects the eigenstates to be delocalized independently of the density of instantons (analogous to the number of impurities which determines the disorder strength). Indeed in a recent paper [19] we showed that an effective random matrix model incorporating the phenomenological power-law decay for the matrix elements of the QCD Dirac operator in a basis of zero modes describes the spectral correlations of the QCD Dirac operator well beyond the Thouless energy $E_c \sim F_\pi^2 / (|\langle \bar{\psi} \psi \rangle| L^2)$ (F_π is the pion decay constant and L the length of the system) which sets the limit of applicability of standard chiral random matrix theory [13]. However at high temperatures, QCD becomes effectively three dimensional, the chiral symmetry is restored and we expect to see localized states appear in the spectrum. One of the main aims of this paper is precisely to investigate the relationship between the vanishing of the chiral condensate and the localization of the eigenstates of the QCD Dirac operator in a background of instantons.

C. ILM at finite temperature: chiral phase transition and localization

In this section we summarize how the ILM is extended to finite temperature and also to what extent reproduces the main features of QCD at temperatures around the chiral phase transition. It is clear that for sufficiently high temperature (beyond the chiral phase transition) QCD becomes perturbative and instanton configurations should be exponentially suppressed. However at temperatures around and below the chiral phase transition the density of instantons is still large and it is expected that they play an important role in the description of the phase transition. The generalization of the ILM to finite temperature was presented in [6]. Below we provide a brief summary of its main features and refer to [6] for details:

- The effective coupling constant $g(T)$ decreases (QCD is an asymptotically free theory) as temperature increases. The density of instantons ρ decreases with temperature since $\rho \propto \exp(-S)$ with $S = 8\pi^2/g^2(T)$. At the restoration temperature the density is still roughly half of the zero temperature value.
- Instanton like solutions (usually called calorons) are still zero modes of the QCD Dirac operator at finite temperature. However the decay of the associated fermionic zero mode $\psi(R) \sim e^{-\pi TR}$ (R is the 3D instanton–anti-instanton distance) is exponential (instead of power-law) in the spatial dimensions and oscillatory in the Euclidean time dimension.
- The probability $|T_{IA}| \sim e^{-\alpha TR}$ (α a numerical factor of order unity) for a fermionic zero mode to hop from an instanton to an anti-instanton has an exponential tail in the spatial dimensions thus restricting the overlap only to nearby instantons. On the contrary, in the time direction the probability is oscillatory. This suggests that at finite temperature the isolated fermionic zero modes are exponentially localized in space but delocalized in time, thus for localization studies the dimension of the system is three and not four. In this case, since the effective hopping is short range, the global localization properties of the eigenstates of QCD Dirac operator are expected to depend strongly on the density of instantons as for normal disordered conductors in 3D.
- The exponentially small tail of the overlap matrix elements together with the oscillatory behavior in Euclidean time suggest that in the high temperature limit (higher than the restoration temperature) the instantons and anti-instantons are paired in molecules aligned along the time direction. As a consequence the spectral density of the QCD Dirac operator develops a gap near zero making, according the Banks-Casher relation, the chiral condensate vanish.

Although certainly appealing, the validity of the ILM at finite temperature as an accurate model for QCD around the phase transition should be corroborated by lattice simulations. Recent lattice studies [20] suggest that this is the case though further investigations are needed to fully settle this issue.

D. Anderson transition: description and signatures

A disordered system with short range hopping in three or more dimensions displays a metal-insulator transition or Anderson transition (AT) around the band center for a critical amount of disorder. By critical amount of disorder we mean if the disorder is increased all the eigenstates become exponentially localized. For a disorder strength below the critical one, the system has a mobility edge at a certain energy which separates localized from delocalized states. Its position moves away from the band center as the disorder is decreased. Delocalized eigenstates, typical of a metal, are extended through the sample and the level statistics agree with the random matrix prediction for the appropriate symmetry. In this paper we will focus on QCD with three colors which corresponds to random matrix predictions from the Gaussian Unitary Ensemble (GUE) [21]. The level statistics obtained from random matrix theory are also referred

to as Wigner-Dyson statistics (WD). On the contrary, localized eigenstates, typical of an insulator, are characterized by an exponential decay $|\psi(r)| \sim e^{-r/\xi}$ with the localization length ξ smaller than the system size. The spectral correlations in this case are well described by Poisson statistics [21] corresponding to uncorrelated eigenvalues.

Around the mobility edge the system is referred to as being at the AT (or at the metal-insulator transition). Signatures of this transition are found in both the spectrum and the eigenfunctions. The eigenstates are multifractal, namely, the wavefunction moments $P_q = \int d^d r |\psi(r)|^{2q} \propto L^{-D_q(q-1)}$ present anomalous scaling with respect to the sample size L , where D_q is a set of different exponents describing the transition [22, 23]. The second moment P_2 is usually referred to as the inverse participation ratio (IPR). Despite the fact that multifractal eigenstates occupy a vanishing volume, they strongly overlap each other. For instance, the density-density correlation function of two eigenstates with energies E_n and E_m decay as a power-law,

$$\int d^d r |\psi_n(r)|^2 |\psi_m(r)|^2 \sim |E_n - E_m|^{-[1-(D_2/d)]} \quad (4)$$

(for a review see [17, 23]).

Level statistics at the AT are universal and intermediate between WD and Poisson statistics. Typical features include:

1. A scale invariant spectrum [24] such that any spectral correlator utilized to describe the spectral properties does not depend on the system size. We recall that, according to the one parameter scaling theory of localization, the AT occurs when the disorder strength is such that the conductance is size independent (the beta function has a zero).
2. Level repulsion such that the nearest neighbor level spacing distribution, $P(s)$, (which gives the probability of having two eigenvalues at a distance s) vanishes as $s \rightarrow 0$, thus adjacent levels still repel each other as in metallic samples. However $P(s) \sim e^{-As}$ for $s \gg 1$, similar to the result for an insulator $P(s) = e^{-s}$ though the constant A is always larger than the unity (~ 1.7 at the 3D Anderson transition).
3. Long range correlators such as the number variance $\Sigma^2(\ell) = \langle (N_\ell - \langle N_\ell \rangle)^2 \rangle \sim \chi \ell$ for $\ell \gg 1$ are asymptotically linear [25], as for an insulator $\Sigma^2(\ell) \sim \ell$, but with a slope $\chi < 1$ ($\chi \sim 0.27 \pm .02$ for a 3D Anderson model). Here N_ℓ is the number of eigenvalues in an interval of length ℓ . Likewise the spectral rigidity (a smoothed version of the number variance) given by $\Delta_3(\ell) = \frac{2}{\ell^4} \int_0^\ell (\ell^3 - 2\ell^2 x + x^3) \Sigma^2(x) dx$ is also linear with slope $\Delta_3(\ell) \sim (\chi/15)\ell$.

The above discussion, with small modifications, holds independently of the details of the microscopic disorder distribution or whether the system has any additional symmetries. Our case of interest, the QCD Dirac operator, has an additional chiral symmetry which makes the matrix representing the operator have a block structure given in equation (2). Obviously the additional chiral symmetry does not affect the properties in the bulk of the spectrum but certainly may have an impact on the eigenvalues close to the origin. It turns out that in this region [15, 26, 27] the properties of the eigenstates depend strongly on the dimension of the space and the disorder distribution. For instance for a 3D disordered system with chiral symmetry and short range (nearest neighbor) disorder [26, 27] the eigenvectors are power-law localized with an exponent depending on the density of impurities. Typically, in lower dimensions (1D,2D) eigenvectors close to the origin are more delocalized than those at the bulk. The reasons for such anomalous behavior have been traced back [28] to the absence of weak-localization corrections in the chiral case. By contrast in three dimensions, it has been claimed [26] that eigenstates close to the origin are more localized than those in the bulk for a broad range of disorder strengths. However there is no consensus on whether this finding is universal or it is just a peculiarity of the model utilized in [26]. In any case it is expected that, for a certain disorder strength, an AT close to the origin may coexist with the one above reported at the bulk. Indeed, this is also what we have found in the ILM at finite temperature (see next section). Clearly further investigation is still needed to provide a detailed account of the AT close to the origin in disordered systems with chiral symmetry.

In summary, at zero temperature certain features of the QCD vacuum resemble those of a disordered medium where the role of impurities is played by an instanton liquid. The S_χ SB is a consequence of the delocalized nature of the zero mode eigenvectors of the QCD Dirac operator caused by the long range nature of the overlap matrix. A natural question to ask is whether these analogies can be extended to the case of finite temperature. The aim to this paper is to answer affirmatively this question. Specifically, in the context of an Instanton Liquid Model, we show that around the temperature that the chiral phase transition occurs the low lying eigenmodes of the QCD Dirac operator undergo an Anderson transition, characterized by multifractal eigenstates and critical statistics [2].

II. ANDERSON LOCALIZATION IN THE ILM AT FINITE TEMPERATURE

In this section we show that both the spectrum and the eigenvectors of the QCD Dirac operator in an ILM undergo a transition to localization at a certain temperature. Both the quenched and the unquenched cases are considered here. In the latter case we see that the transition to localization occurs around the same temperature as the chiral phase transition thus suggesting that both phenomena are deeply related. This is the main result of this paper. First we provide a short overview on how the numerical simulations were performed.

A. Technical details of the numerical simulation

The ILM partition function for N_f quark flavors with masses m_k is given by

$$Z_{\text{inst}} = \int D\Omega e^{-S_{\text{YM}}} \prod_{k=1}^{N_f} \det(\not{D} + m_k), \quad (5)$$

where the integral is over the positions, sizes and orientations of the instantons and S_{YM} is the Yang-Mills action. The fermion determinant is evaluated in the space of the fermionic zero modes of the instantons. For further discussion of this partition function we refer to [6]. We just mention that we use the standard phenomenological value of the instanton density $N/V = 1 \text{ fm}^{-4}$. For the sake of simplicity we have kept this density fixed as the temperature is increased. We justify this approximation based on the fact that even for temperatures close to the chiral phase transition the instanton density is still sizable (around 0.6 fm^{-4} [6]). Indeed in previous simulations the drop in the density was ruled out as the physical mechanism leading to the chiral phase transition [6].

All units in the ILM are typically given in terms of the QCD scale parameter Λ which we have simply set to 200 MeV. This choice is sufficient for our purposes since we are not concerned with making quantitative predictions about the position of the QCD chiral phase transition, but instead are interested in more general features of the transition that we don't expect to be very sensitive to a fine tuning of the parameters of the ILM. We therefore use the ILM as a qualitative model for QCD at temperatures around the chiral phase transition. We also stress that it provides a reasonable description of $S_{\chi\text{SB}}$ and many hadronic correlation functions both at zero and at finite temperature. Furthermore the ILM has modest computational requirements and allows us to go to fairly large volumes and get good statistics.

In this paper we present results for both the quenched $N_f = 0$ and the unquenched $N_f = 2, 3$ cases ($N_f = 2$ with $m_u = m_d = 0$ and at $N_f = 3$ with $m_u = m_d = 20 \text{ MeV}$ and $m_s = 140 \text{ MeV}$). The partition function, equation (5), is evaluated using a standard Metropolis algorithm. In the quenched case we performed between 2000 to 10000 measurement sweeps for each set of parameters after allowing around 1000 sweeps for thermalization. Results are presented for ensembles of up to $N = 5000$ instanton and anti-instantons. In the unquenched case we were only able to investigate ensembles of up to $N = 700$ instantons and anti-instantons. We also discarded the first 1000 sweeps in each simulation and did between 1000 to 5000 sweeps per ensemble. Thermodynamic properties of the model have already been addressed in [6] and will not be discussed here. We will focus mainly on observables such as level statistics and eigenvector scaling properties of the QCD Dirac operator which are especially well suited for studying Anderson localization effects [23]. All the spectral correlators are calculated from the unfolded spectrum. This procedure scales the eigenvalues so that the spectral density on a spectral window comprising several level spacings is unity but it does not remove the small fluctuations about the mean density that provide fundamental information about the system.

Finally we recall that in the ILM the effective disorder parameter is the temperature since we have fixed the density of instantons. One of the most challenging tasks of the numerical calculation is to accurately locate the temperature at which the AT occurs. In all cases in the paper this temperature has been estimated by the finite size scaling method introduced in [24] in the context of disordered systems. In essence this method consists of computing a spectral correlator, such as the level spacing distribution $P(s)$ or the number variance $\Sigma^2(\ell)$, for different sizes and then finding the temperature at which it becomes size independent.

B. Anderson localization in the ILM: The quenched case

In this section we present results for the quenched ILM at nonzero temperature. Without dynamical fermions there is not technically a chiral phase transition since there is no chiral symmetry. However one can in principle study the “quenched” quark condensate in a purely gluonic background through the Banks-Casher relation [9]. Lattice simulations with staggered fermions [1] have also found that the vanishing of the “quenched” quark condensate

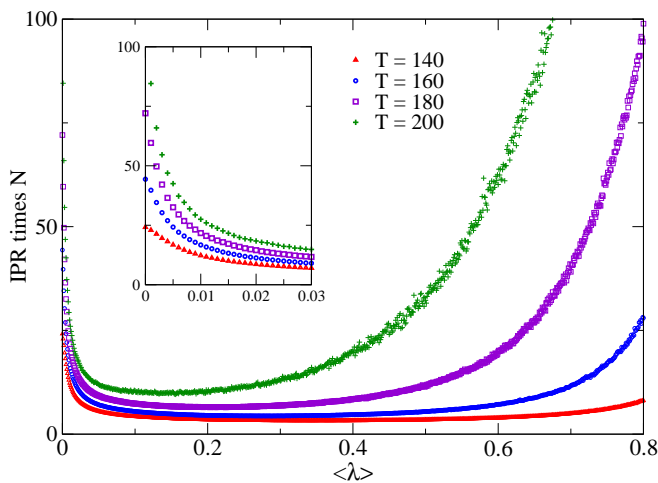


FIG. 1: Inverse participation ratio (IPR) times N versus the average eigenvalue for the quenched ILM with $N = 2000$ instantons at different temperatures. Low lying eigenmodes are more localized than those in the bulk for all tested temperatures.

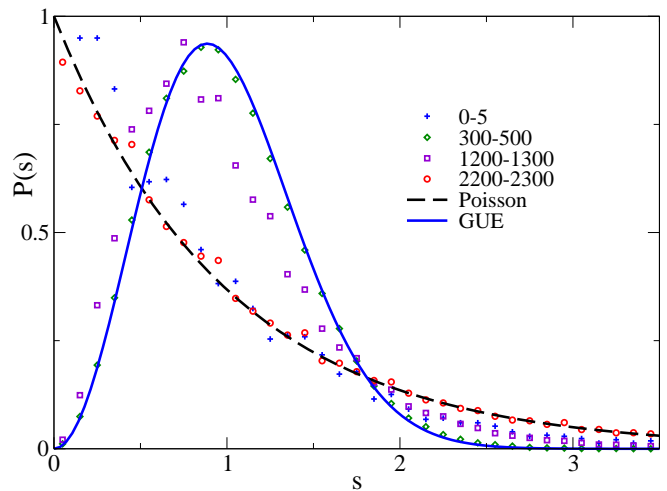


FIG. 2: Level spacing distribution $P(s)$ for the quenched ILM with $N = 5000$ instantons at $T = 200$ MeV for different spectral windows. The legend indicates the eigenvalue numbers with 0 being the smallest one. The spectral correlations of the lowest and highest modes are close to Poisson statistics. By contrast the spectral correlations in the central part of the spectrum are well described by RMT (GUE result).

occurs at the same temperature as the deconfinement transition does. Since the ILM does not have a confinement-deconfinement transition [6] we can only speak about the chiral phase transition in the ILM. However, in the quenched ILM, the spectral density seems to diverge close to the origin (similarly to recent lattice results with overlap fermions [29]) thus suggesting a likewise divergent “quenched” quark condensate. In view of these facts the transition to localization (see below) we have observed in the quenched QCD Dirac operator at finite temperature both close to origin and in the bulk of the spectrum can’t be linked directly to either of these phenomena. We still consider the quenched ILM results to be of interest as we have found a very clear example of a mobility edge with features strikingly similar to those of a 3D disordered system at the AT. This finding reinforces the idea [19] that certain aspects of the QCD vacuum resemble those of a disordered system.

We start by summarizing our main findings:

1. The eigenvectors of the QCD Dirac operator at finite temperature with the lowest eigenvalues (the origin) are much more localized than the ones in the middle of the spectrum (the bulk). Signs of stronger localization close to the origin were observed not only in the eigenvector moments (figure 1) but also in the level statistics (figure 2). This difference between the origin and bulk has also been reported in 3D disordered systems with chiral symmetry [26].
2. In the bulk we find a mobility edge separating localized from extended states which moves toward the high end of the spectrum as the temperature is decreased. The level statistics of eigenstates around the mobility edge are well described by critical statistics (see figures 3 and 4) typical of a 3D disordered conductor at the AT. Outside the critical region the level statistics are similar to those of a metal (Wigner-Dyson statistics) in the region below the mobility edge. By contrast, in the region above the mobility edge, it resembles those of an insulator (Poisson statistics).
3. Close to the origin we observe a transition to localization for temperatures in the range $T \sim 100 - 140$ MeV (see figure 5).

1. The bulk

Using the finite scaling method introduced in [24] we found a mobility edge in the bulk of the spectrum in the range $T \sim 150 - 250$ MeV. As the temperature decreases its location moves to the end of the spectrum. For $T < 170$ MeV the results are less reliable since the mobility edge is located almost at the end of the spectrum where truncation effects due to the finite size of the ILM are larger. Following the literature in disordered systems we have investigated

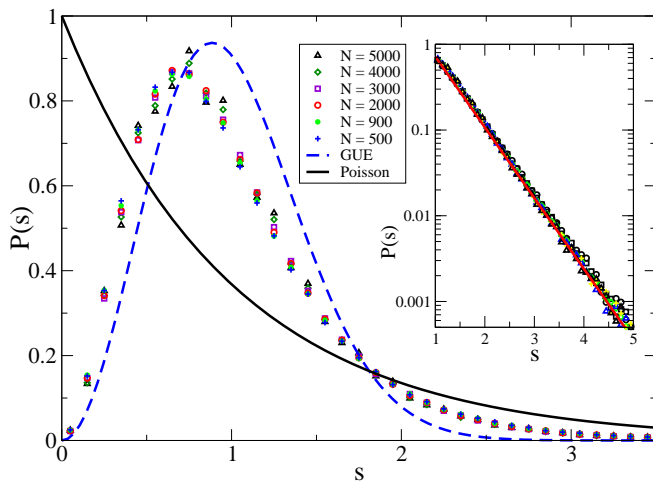


FIG. 3: Level spacing distribution $P(s)$ in the bulk of the spectrum for the quenched ILM at $T = 200$ MeV and different numbers of instantons. The inset shows the tail of $P(s)$. The solid line corresponds to the best fit $P(s) \sim e^{-1.86s}$.

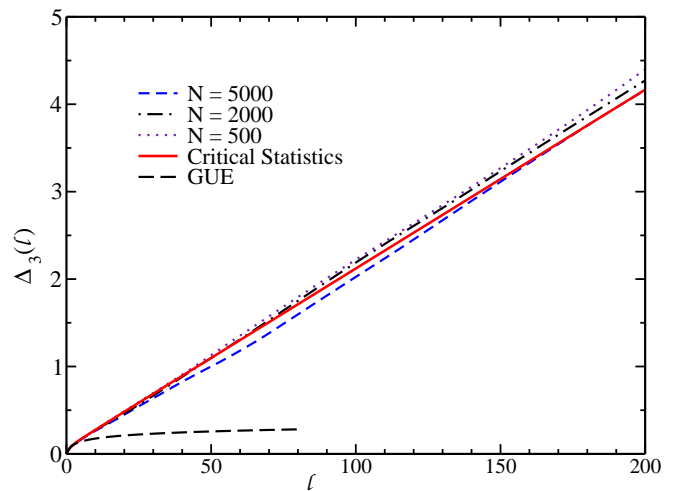


FIG. 4: Spectral rigidity $\Delta_3(\ell)$ in the bulk of the spectrum for the quenched ILM at $T = 200$ MeV and different numbers of instantons. The result is almost size independent and agrees well with the prediction of critical statistics (solid line).

the temperature $T \sim 200$ MeV such that the mobility edge is located around the center of the spectrum. We initiate our analysis by looking at the level statistics. We recall the spectral correlators were computed from the unfolded spectrum in the region around the mobility edge. The main findings are summarized as follows:

1. The spectrum is scale invariant to high degree. As observed in figure 3, the level spacing distribution $P(s)$ does not depend much on the system size for volumes ranging from $N = 500$ to $N = 5000$. The inset plot shows that even the tail of $P(s)$ which contains information about correlations at larger scales is also scale invariant. The study of long range correlators further confirms this behavior. Likewise, in figure 4, it is shown that the spectral rigidity varies little with the system size in a window of more than 200 eigenvalues around the mobility edge.
2. Level repulsion, $P(s) \rightarrow 0$ as $s \rightarrow 0$, typical of a metal is still present (figure 3). However $P(s) \sim e^{-1.86s}$ has an exponential tail as for an insulator. Both features also appear in the case of a 3D disordered system at the AT.
3. The spectral rigidity (figure 4) is asymptotically linear with a slope $\chi/15 \sim (0.29 \pm 0.02)/15$ in fair agreement with the result of a 3D disordered system at the AT of $\chi \sim 0.27/15$ [23].
4. The level statistics of the ILM in the critical region are accurately described by generalized random matrix models [30, 31] capable of reproducing critical statistics (see figure 4). The explicit analytical result for the chiral case can be found in [32] for a random banded model with a power-law decay and in [31, 33] in the context of the Calogero-Sutherland model [34] at finite temperature. We recall that in these models there exists a free parameter that must be fixed by, for instance, matching the slope of the spectral rigidity χ . In our case, as shown in figure 4, the exact form of the spectral rigidity in the bulk follows closely the prediction of critical statistics, equation (31) in [31] with h , a free parameter, set to a value of 0.62.
5. The level statistics outside the AT window are given by Wigner-Dyson statistics (typical of a metal) in the region below the mobility edge. By contrast it is close to Poisson statistics typical of an insulator in the region above the mobility edge. This is corroborated in figure 2 where we observe a transition from Poisson to Wigner-Dyson statistics in $P(s)$ at $T = 200$ depending the region of the spectrum where $P(s)$ is computed.

The above analysis provides compelling evidence that for a certain range of temperatures the level statistics in the bulk of the QCD Dirac operator in the ILM are consistent with those of a 3D disordered system at the AT.

We now turn to eigenvector properties. As mentioned previously, a signature of the AT is the multifractality of the eigenstates. Multifractality is usually detected by the anomalous scaling of the moments of the eigenfunction P_q (defined in section ID) with the system size $L \propto N^{1/3}$. We have computed the fractal dimension D_2 by fitting P_2 for different system sizes N . A fit to the form $P_2 = aN^b$ yields $b \sim 0.50(5)$ and consequently $D_2 \sim 1.5(1)$, consistent with the $D_2 \sim 1.4(2)$ found for a disordered system at the 3D AT. In order not to consider eigenstates outside the critical region we have taken only 10% of the eigenvectors around the center of the spectrum.

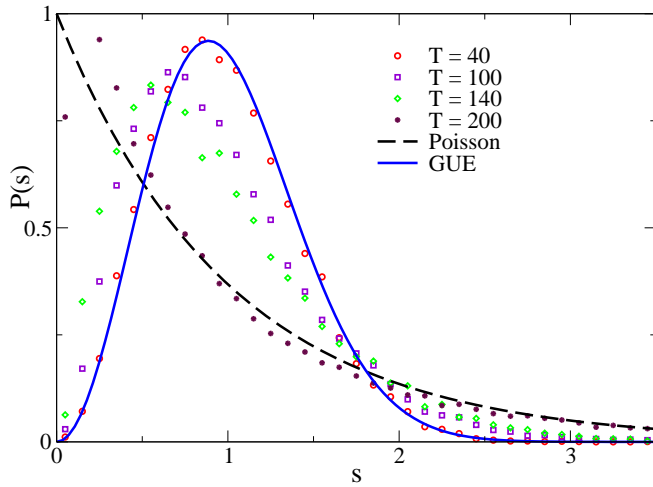


FIG. 5: Level spacing distribution $P(s)$ close to the origin of the spectrum for the quenched ILM with $N = 2000$ instantons for different temperatures. Agreement with the prediction of RMT (GUE result) is observed for relatively low temperatures $T < 100$ MeV. A transition between RMT (GUE) and Poisson statistics is observed in the range $T \sim 100 - 140$ MeV.

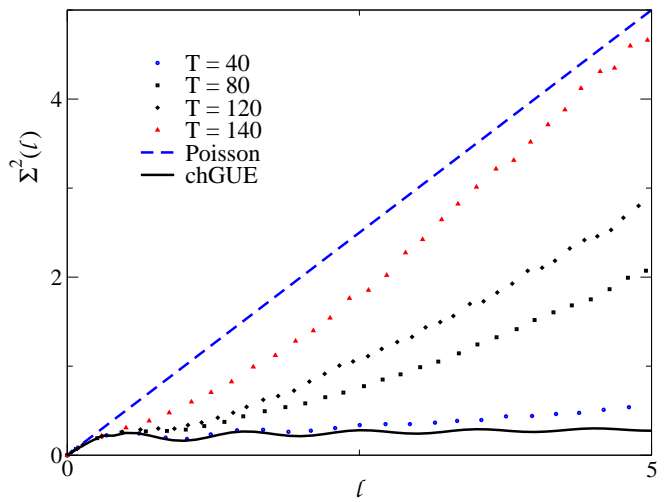


FIG. 6: Number variance $\Sigma^2(\ell)$ at the origin for the quenched ILM with $N = 1600$ instantons for different temperatures. Agreement with the RMT (chiral GUE) result is observed for relatively low temperatures $T < 80$ MeV. The temperature range of the transition to Poisson agrees with that obtained from the level spacing distribution.

To recapitulate, the numerical analysis shows with great accuracy that at $T = 200$ MeV the QCD Dirac operator in a background field given by the quenched ILM undergoes a metal-insulator transition in the central part of the spectrum. The eigenstates around the transition region are fractal and the level statistics are well described by critical statistics, namely, they have all the properties expected in an AT: scale invariance, level repulsion and sub-Poisson spectral rigidity. Furthermore the numerical value of parameters such as the fractal dimension D_2 and the slope of the number variance χ are very close to the results for a standard 3D disordered system at the AT.

2. The origin

This region is of special interest since the smallest eigenmodes are responsible for $S\chi$ SB. However as mentioned earlier, in the quenched case there is not, in a strict sense, chiral symmetry so the localization properties in this region cannot be related neither to $S\chi$ SB nor its restoration at finite temperature. Despite these limitations we have also investigated both the spectrum and the eigenmodes in this region. Our main motivation is to test whether the similarities between the QCD vacuum (as given by the ILM at a certain temperature) and a 3D disordered system at the AT can also be extended to region close to the origin thus reinforcing the idea put forward in [19] that both models belong to the same universality class.

As in the bulk, the level statistics are temperature dependent. For low temperatures $T < 80$ MeV (see figures 5 and 6), the eigenmodes are delocalized and the level statistics are very close to the RMT prediction as given by the GUE. In the region $T \sim 100 - 140$ MeV we observe a transition to localization. By contrast at higher temperatures the spectrum is very nearly Poisson like as for an insulator.

We remark that the numerical results close to the origin are less conclusive than those in the bulk. On the one hand the analysis is complicated by the accumulation of very small eigenvalues present in the quenched ILM. On the other hand the statistics are worse since only the smallest eigenvalues are affected by the chiral symmetry of the model. Despite these technical problems it seems clear that the QCD Dirac operator undergoes a transition to localization for $T \sim 120$ MeV. As shown in figure 1, eigenvectors for the smallest eigenvalues, due to the additional chiral symmetry, are more localized than those in the bulk. This has already been observed in lattice simulations [20, 35] and 3D disordered systems with chiral symmetry [26]. We do not have a clear understanding of the reason for such behavior. Indeed 1D and 2D chiral disordered models usually show the opposite behavior, namely, states in the bulk are localized for any amount of disorder and only the states close to the origin (the ones affected by the chiral symmetry) are truly delocalized.

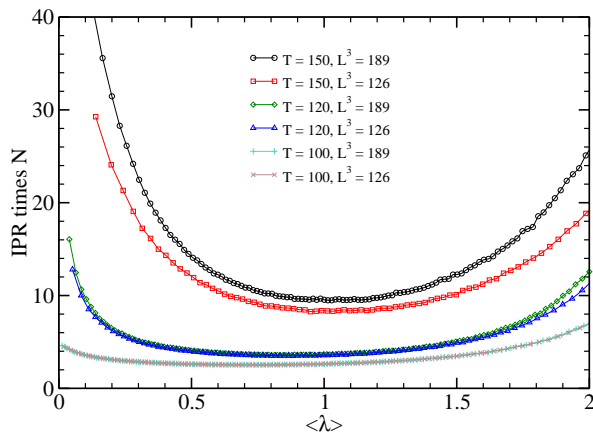


FIG. 7: IPR times the total volume ($V = N$ in units of fm) versus the average eigenvalue for the ILM with 2 massless quarks at different temperatures and spatial volumes (L^3 , in units of fm 3).

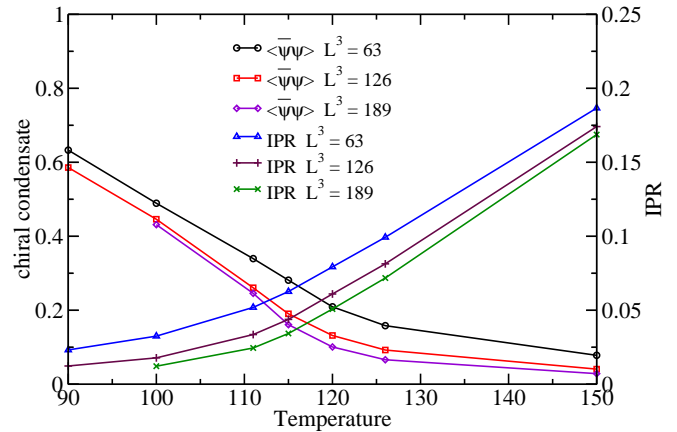


FIG. 8: Chiral condensate $\langle \bar{\psi}\psi \rangle$ and the IPR of the lowest eigenmode versus temperature for the ILM with 2 massless quarks at different spatial volumes (L^3 , in units of fm 3). Remarkably the drop in the condensate occurs in the same range of temperatures as the transition to localization of the lowest eigenmodes of the QCD Dirac operator.

C. Anderson transition and chiral phase transition: The unquenched case

In this section we investigate the eigenvalue and eigenvector statistics of the QCD Dirac operator with two massless quark flavors and for three flavors with $m_u = m_d = 20$ MeV and $m_s = 140$ MeV. In the massless case a true chiral phase transition is supposed to occur at a certain (chiral restoration) temperature. Our main aim is to investigate whether the chiral phase transition and the localization transition in the QCD Dirac operator occur at the same temperature. Below we show that this is indeed the case thus suggesting that the phenomenon of Anderson localization may be the fundamental mechanism driving the chiral phase transition.

We mention that in the massive case there is not a chiral phase transition but instead a crossover as is believed to occur in full QCD. The quark masses have been chosen larger than the experimental values in order to observe this crossover in the ILM. Additionally such large mass values are closer to the ones typically used in current lattice calculations.

The behavior of the ILM at finite temperature for different numbers of flavors has been studied previously [36]. The case of just one flavor $N_f = 1$ is special since the chiral symmetry is explicitly broken by the $U(1)$ anomaly, a condensate is formed but is not related to the spontaneous breaking of any symmetry. This condensate decreases smoothly with the temperature and there is no sign of any phase transition [36]. By contrast for $N_f > 5$ the chiral symmetry is no longer broken (in the chiral limit) at zero temperature. This is due to the fact that the fermionic determinant in the partition function suppresses configurations with low-lying eigenvalues. The rate of suppression increases with the number of flavors as λ^{N_f} . It is believed that for $N_f \sim 5$ the spectral density of the Dirac operator develops a gap close to the origin and, by the Banks-Casher relation, the chiral symmetry is not broken even at zero temperature.

We start our analysis with the eigenmode properties of the QCD Dirac operator with two massless flavors. In figure 7 we show the IPR times the total volume V (or number of instantons N) versus the average eigenvalue for different temperatures and spatial volumes. Completely extended states will have a constant $\text{IPR} \times V$ independently of the system size, while for completely localized states $\text{IPR} \times V$ will be proportional to the volume. As in the quenched case eigenstates close to the origin are more localized than those in the bulk but the difference between the two regions is smaller than in the quenched case. This is not surprising since the fermionic determinant suppress low-lying eigenvalues thus weakening the chiral symmetry and consequently the difference between the origin and bulk. At the lowest temperature ($T = 100$ MeV) we clearly see that the scaled IPR is independent of the volume and consequently the eigenmodes are delocalized. The opposite occurs for $T = 150$ MeV where scaling is observed in all eigenmodes, especially the ones close to the origin, indicating that the eigenmodes are localized. An intermediate situation happens at $T \sim 120$ MeV where we see some volume dependence near the origin and at the high end of the spectrum while the bulk states remain fairly constant. This indicates that a mobility edge separating localized from delocalized states is forming at the origin. A natural question to ask at this point is whether this transition to localization occurs in the same range of temperatures as the chiral phase transition.

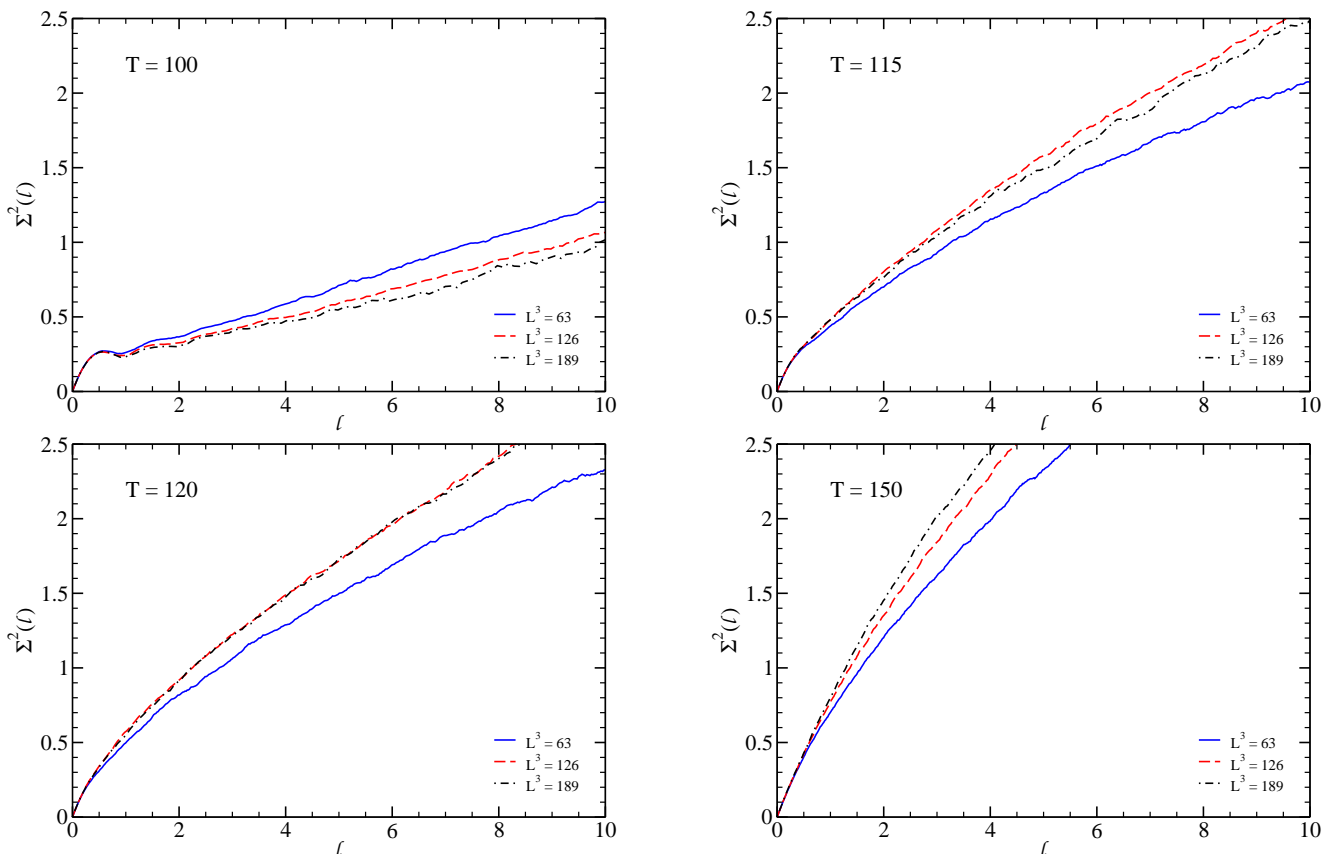


FIG. 9: Number variance $\Sigma^2(\ell)$ at the origin for the ILM with two massless quark flavors at different temperatures and spatial volumes (L^3 , in units of fm^3). The scaling with volume is very small for $T \sim 120$ MeV which indicates that the critical temperature associated with the AT is very close.

In figure 8 the chiral condensate versus temperature is shown for a range of system sizes. We see that the condensate decreases as the temperature is increased in a manner consistent with a second order phase transition. Although we would need to go to much larger volumes to determine the transition temperature more accurately there is a clear bend in the condensate around a temperature of $T_c \sim 120$ MeV which indicates that the chiral phase transition should occur around this region. Remarkably, as shown in figures 7 and 8, this is also around the temperature at which the IPR of the lowest eigenmode begins to rise signaling a transition to localization. This finding suggests that both transitions could be intimately related. Indeed it shows that the phenomenon of Anderson localization may be the fundamental mechanism leading to the chiral phase transition in QCD. In order to further confirm that this novel relation between QCD and the theory of disordered system is not a peculiarity of the ILM utilized in this paper we are currently carrying out similar numerical calculations in the framework of lattice gauge theory [37]. We stress that the relation between an Anderson transition and the chiral phase transition is the main result of this paper.

We now turn to the level statistics. In order to locate the localization transition temperature more precisely we look at the number variance $\Sigma^2(\ell)$ near the origin. In figure 9 we plot this for different temperatures and spatial volumes. At $T = 100$ MeV, the number variance decreases as the system size increase thus indicating that the states are still extended at this temperature. At $T = 120$ MeV there is still a big difference between the smallest volume ($L^3 = 63 \text{ fm}^3$) and the larger ones, but the two larger volumes fall directly on top of each other. We believe that this is very near the localization transition and that the smaller volume is just too small to reliably see the proper scaling. For higher temperatures $T \sim 150$ MeV the number variance moves rapidly towards the prediction of Poisson statistics $\Sigma^2(\ell) = \ell$, typical of an insulator.

We observe a similar picture for short range spectral correlators such as $P(s)$. For a fixed volume the spectral correlations diminish as we increase the temperature. Thus the level spacing distribution moves (see figure 10) from the RMT result (GUE) typical of a metal to Poisson statistics typical of an uncorrelated spectrum. By fixing the temperature at 120 MeV and looking at the spatial volume dependence (figure 11) of $P(s)$, we observe very little difference for the range of sizes considered in agreement with the results for the number variance. We also see that there is still level repulsion but the tail of $P(s)$ is exponential as for an insulator. All these features are typical

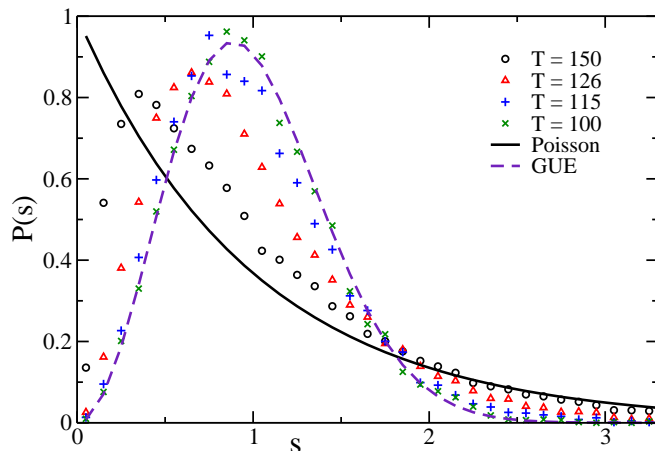


FIG. 10: Level spacing distribution $P(s)$ at the origin for the ILM with 2 massless quarks with spatial volume $L^3 = 189 \text{ fm}^3$ for different temperatures. A transition from the RMT prediction (GUE) typical of a metal to the Poisson result typical of an insulator is observed as the temperature is increased.

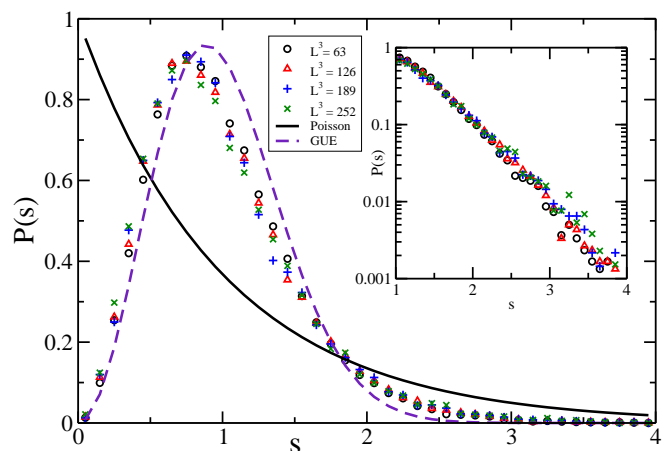


FIG. 11: Level spacing distribution $P(s)$ at the origin for the ILM with 2 massless quarks at the critical temperature $T_c = 120 \text{ MeV}$ for different spatial volumes. The scale invariance indicates the system is undergoing an AT.

signatures of an AT.

The AT is also characterized by the multifractality of the eigenstates. We investigate this feature by looking at the scaling of $P_q \sim L^{-D_q(q-1)}$ for low eigenvalues at $T = 120 \text{ MeV}$ for system sizes ranging from $L^3 = 63\text{--}252 \text{ fm}^3$. The resulting fractal dimensions D_q are shown in table I for an eigenvalue of $\langle \lambda \rangle = 0.076$ which is the smallest eigenvalue for the $L^3 = 63$ data. The IPRs for the remaining sizes were interpolated to this eigenvalue (see figure 7). We clearly see D_q change with q thus showing that the eigenstates are truly multifractal. It is worth mentioning that the numerical value of D_q is very sensitive to small temperature changes. Thus at $T = 111 \text{ MeV}$ we find that $D_2 = 3.07(5)$ like for a metal ($D_2 = 3$) but at $T = 150 \text{ MeV}$, $D_2 = 0.96(4)$ which is closer to the value for an insulator ($D_2 = 0$).

Just in passing we mention that a mobility edge and the corresponding AT has also been found in the bulk of the spectrum. As in the quenched case, the temperature at which it appears in the central part of the spectrum is higher than the one close to the origin. This is consistent with the picture that, at a fixed temperature, eigenvectors close to the origin are more localized than those in the bulk of the spectrum. Indeed similar results have also been obtained in lattice calculations [20, 35]. The eigenvalue and eigenvector statistics are also similar to the results shown for the quenched case at the AT so we will not present them here.

Finally we discuss the case of the $N_f = 3$ ILM with masses $m_u = m_d = 20 \text{ MeV}$ and $m_s = 140 \text{ MeV}$. As a general comment we observe strong similarities with the quenched and $N_f = 2$ cases studied previously. Thus, as the plot of the level spacing distribution $P(s)$ in figure 12 shows, the lowest eigenmodes move from extended (metal) to localized (insulator) as the temperature is increased.

More importantly, we have also found that the the localization transition of the low-lying eigenmodes of the QCD Dirac operator occurs around the same temperature $T_c \sim 125 \text{ MeV}$ as the crossover to the chirally symmetric phase (which is also not far from the value for two massless flavors). However we remark that since the lightest masses were still fairly large the eigenvalue density increases at the origin like in the quenched case and in lattice simulations with overlap fermions [29]. Even though the chiral condensate only signals a crossover we still see evidence of critical statistics in the critical region $T_c \sim 125 \text{ MeV}$. Thus, as shown in figure 13, the level spacing at the origin is scale invariant and exhibits level repulsion at small distances while having an asymptotically exponential tail.

q	2	3	4	5
D_q	2.67(4)	2.34(5)	2.08(6)	1.87(7)

TABLE I: Fractal dimensions (D_q) for the ILM with 2 massless flavors at $T = 120 \text{ MeV}$.

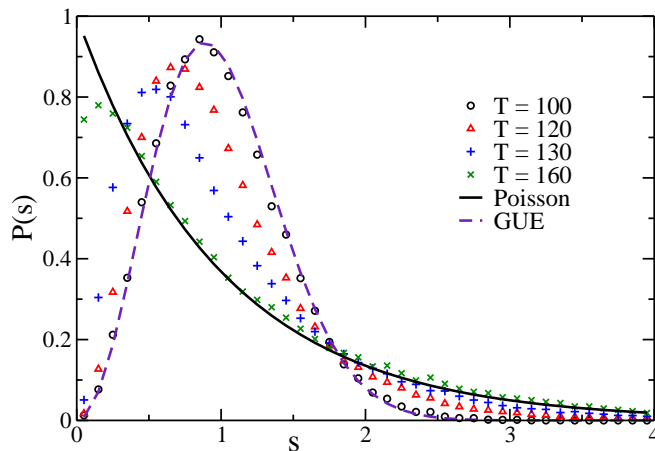


FIG. 12: Level spacing distribution $P(s)$ at the origin for the ILM with $N = 300$ instantons and 3 massive flavors at different temperatures. As in previous cases a transition to localization is observed as the temperature is increased.

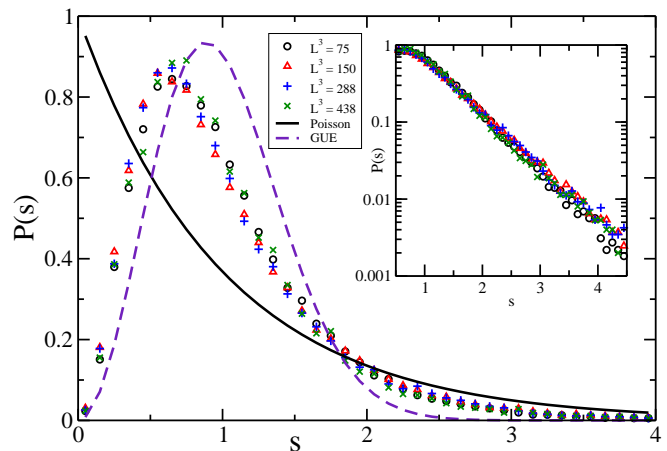


FIG. 13: Level spacing distribution $P(s)$ at the origin for the ILM with 3 massive flavors at $T = 125$ MeV for different spatial volumes. The spectrum is nearly scale invariant as expected at an AT.

III. DISCUSSION AND RELATION TO LATTICE RESULTS

In this section we investigate to what extent the relation between Anderson transition and chiral phase transition reported in previous sections is a particularity of the ILM or could be a real feature of the strong interactions. Obviously a conclusive answer to this question can only be given after a full analysis [37] of the QCD Dirac operator around the restoration temperature is carried out in a direct simulation of QCD on a lattice.

However it is instructive to clearly establish the reasons for the appearance of the AT in the ILM. As is known, the fermionic zero modes in the field of an instanton at nonzero temperature have an exponential tail e^{-rT} in the spatial directions and are oscillatory in the time direction [6]. This suggests that the overlap among different zero modes is essentially restricted to nearest neighbors in the spatial directions. However, in the time direction, different zero modes strongly overlap due to the oscillatory character of the eigenmodes. This situation strongly resembles a 4D disordered conductor in the tight binding approximation (only nearest neighbor hopping) with one dimension (time) much smaller than the rest so the system can be considered effectively three dimensional. It is well established that such a system may undergo an AT depending on the disorder strength. In our case the disorder role is played by temperature since the low-lying eigenvectors of the QCD Dirac operator decay as $\sim e^{-rT}$. From this discussion it is natural to find an Anderson transition in the ILM for a particular value of the temperature. The principal ingredient to reach the AT is an exponential decay of the eigenmodes explicitly depending on the temperature together with the possibility to tune the effective range of the exponential in order to reach the transition region. Any theory with these features very likely will undergo an AT for some value of the parameters even if the objects responsible for localization are not the classical instantons. In fact this is not the only scenario in which an AT could arise. As mentioned in the introduction, an AT is also expected in the case that at a certain temperature the dominant gauge configurations are such that the resulting low lying eigenmodes are power-law localized $|\psi(r)| \sim 1/r^\alpha$ with $\alpha \sim 3$.

We also remark that the AT in the ILM cannot be induced by instanton–anti-instanton molecules. As the temperature is increased overlapping among different instantons becomes more rare and eventually, in the the high temperature limit, the ILM is composed of independent instanton–anti-instanton molecules. However such situation does not occur at temperatures around the chiral phase transition due to the multifractal character of the eigenstates. In the molecular phase the zero modes are attached to a unique instanton–anti-instanton pair, the wavefunction will be localized in between the two pseudoparticles and consequently the eigenstates cannot be truly multifractal. At most D_q may be a constant not depending on the moment q . Another indication that the molecular phase has not been yet reached at the restoration temperature is the fact that the chiral condensate decreases smoothly over a quite broad range of temperatures. If the molecular phase is dominant a gap appears in the spectral density and the condensate vanishes.

We now discuss the relation of our findings with previous lattice results. Lattice investigations of the QCD Dirac operator at finite temperature have attracted considerable attention in recent years. Results close to the restoration temperature qualitatively agree with the ones reported in this paper. It has been observed [20, 35] that eigenvectors close to the origin are more localized than those of the bulk (see figures 1 and 7). The eigenvalue density of the Dirac operator in the quenched ILM more closely resembles that of lattice simulations of overlap fermions [29] than those of staggered fermions [35]. This is not surprising since the ILM is based on the low energy topological modes that

overlap fermions are supposed to treat accurately while staggered fermions (at large lattice spacing) do not. For two massless flavors the ILM does not have a large eigenvalue density near the origin and we can clearly see the decrease in the condensate as the localization transition occurs. We cannot make a direct comparison to lattice simulations here due to the large cost of simulating massless quarks on the lattice. We also note that a mobility edge has been observed in the low energy modes of Wilson fermions [38] however they do not have a chiral symmetry and we cannot make a direct comparison. In order to further clarify this issue, an updated detailed lattice analysis of level statistics and eigenvectors in the framework of lattice gauge theory would be highly desirable.

Finally we mention that the true nature of the topological objects responsible for $S\chi SB$ and confinement has not been fully settled in lattice QCD. Although there is some support for instanton-like objects there are other studies that suggest a different picture. Recently it has been argued that the topological charge may not be localized in four dimensional regions of space-time but rather spread out over a lower dimensional manifold [39]. The resulting low-lying eigenmodes of the QCD Dirac operator are still delocalized and fractal as we observe in the ILM. This is also not far from the results of the ILM in [13, 19] where it was found that the low-lying eigenmodes are delocalized in the sense that in the thermodynamic limit the level statistics are described by random matrix theory. It would be interesting to compare these predictions with results from overlap fermions at zero temperature.

IV. CONCLUSIONS

We have studied the localization properties of the eigenvalues and eigenvectors of the QCD Dirac operator in a instanton liquid model at finite temperature. Due to the chiral symmetry of the model, eigenstates close to the origin are more localized than those near the center for any temperature. Near the origin we found a clear transition from delocalized to localized states as the temperature is increased. There is also a mobility edge in the bulk of the spectrum that moves toward the region of lower energies as the temperature is increased. In both cases, around this mobility edge, the eigenvectors are multifractal and spectral correlations are well described by critical statistics as for a disordered system undergoing an AT. Remarkably both the transition to localization close to the origin and the chiral phase transition signaling the restoration of the chiral symmetry occur at roughly the same temperature. This suggests that the phenomenon of Anderson localization may be the fundamental mechanism driving the chiral phase transition.

Acknowledgments

AMG thanks Jac Verbaarschot for illuminating discussions. AMG was supported by a Marie Curie Outgoing Fellowship, contract MOIF-CT-2005-007300. JCO was supported in part by U.S. DOE grant DE-FC02-01ER41180.

-
- [1] F. Karsch, E. Laermann and A. Peikert, *Nucl. Phys.* **B605** (2001) 579; C. Gattringer, P.E.L. Rakow, A. Schafer and W. Söldner, *Phys. Rev. D* **66** (2002) 054502.
 - [2] P.W. Anderson, *Phys. Rev.* **109** (1958) 1492.
 - [3] A. Belavin, A. Polyakov, A. Schwartz and Y. Tyupkin, *Phys. Lett.* **59** (1975) 85; G. 't Hooft, *Phys. Rev. Lett.* **37** (1976) 8.
 - [4] D. Diakonov and V. Petrov, *Nucl. Phys.* **B245** (1984) 259.
 - [5] E. Shuryak, *Nucl. Phys.* **B203** (1982) 93,116,140.
 - [6] T. Schäfer and E. Shuryak, *Rev. Mod. Phys.* **70** (1998) 323.
 - [7] T. Shafer, E. Shuryak and J.J.M. Verbaarschot, *Nucl. Phys.* **B412** (1994) 143.
 - [8] M.-C. Chu, et. al., *Phys. Rev. D* **49** (1994) 6039; C. Michael and P.S. Spencer, *Phys. Rev. D* **52** (1995) 4691.
 - [9] T. Banks and A. Casher, *Nucl. Phys.* **B169** (1980) 103.
 - [10] D. Diakonov and P. Petrov, *Phys. Lett.* **B147** (1984) 351; *Nucl. Phys.* **B272** (1986) 457; hep-ph/9602375.
 - [11] A.V. Smilga, *Phys. Rev. D* **46** (1992) 5598.
 - [12] R.A. Janik, M.A. Nowak, G. Papp and I. Zahed, *Phys. Rev. Lett.* **81** 264 (1998).
 - [13] J.C. Osborn and J.J.M. Verbaarschot, *Phys. Rev. Lett.* **81** 268 (1998); *Nucl. Phys.* **B525** 738 (1998).
 - [14] L.S. Levitov, *Phys. Rev. Lett.* **64** (1990) 547; A.D. Mirlin, Y.V. Fyodorov, F.-M. Dittes, J. Quezada and T.H. Seligman, *Phys. Rev. E* **54** (1996) 3221; E. Cuevas, *Phys. Rev. B* **68** (2003) 024206,184206.
 - [15] A. Parshin and H.R. Schober, *Phys. Rev. B* **57** (1998) 10232.
 - [16] V.E. Kravtsov and K.A. Muttalib, *Phys. Rev. Lett.* **79** (1997) 1913; S. Nishigaki, *Phys. Rev. E* **59** (1999) 2853; F. Evers and A.D. Mirlin, *Phys. Rev. Lett.* **84** (2000) 3690; E. Cuevas, M. Ortuño, V. Gasparian and A. Pérez-Garrido, *Phys. Rev. Lett.* **88** (2002) 016401.
 - [17] M. Janssen, *Phys. Rep.* **295** (1998) 1.

- [18] G. Yeung and Y. Oono, *Europhys. Lett.* **4** (1987) 1061.
- [19] A.M. Garcia-Garcia and J.C. Osborn, *Phys. Rev. Lett.* **93** (2004) 132002.
- [20] M. Garcia Perez, A. Gonzalez-Arroyo, A. Montero and P. van Baal, *JHEP* 9906 (1999) 001; M. Göckeler, P.E.L. Rakow, A. Schäfer, W. Söldner and T. Wettig, *Phys. Rev. Lett.* **87** (2001) 042001; C. Gattringer, M. Göckeler, P.E.L. Rakow, S. Schaefer and A. Schäfer, *Nucl. Phys.* **B618** (2001) 205; C. Gattringer and S. Schaefer, *Nucl. Phys.* **B654** (2003) 30; B. Lucini, M. Teper and U. Wenger, *Nucl. Phys.* **B715** (2005) 461; E.-M. Ilgenfritz, M. Müller-Preussker and D. Peschka, *Phys. Rev. D* **71** (2005) 116003.
- [21] M.L. Mehta, *Random Matrices*, Academic Press, New York (1991) 2nd edition.
- [22] F. Wegner, *Z. Phys. B* **36** (1980) 209; B.L. Altshuler, V.E. Kravtsov and I.V. Lerner, in: *Mesoscopic Phenomena in Solids* edited by B.L. Altshuler, P.A. Lee and R.A. Webb, North Holland, Amsterdam, (1991). V.I. Falko and K.B. Efetov, *Europhys. Lett.* **32** (1995) 627;
- [23] A. Mirlin, *Phys. Rep.* **326** (2000) 259.
- [24] B.I. Shklovskii, B. Shapiro, B.R. Sears, P. Lambrianides and H.B. Shore, *Phys. Rev. B* **47** (1993) 11487.
- [25] B.L. Altshuler, I.K. Zharekeshv, S.A. Kotochigova and B.I. Shklovskii, *JETP* **67** (1988) 62.
- [26] B. Nikolic, *Phys. Rev. B* **64** (2001) 014203.
- [27] S. Xiong and S.N. Evangelou, *Phys. Rev. B* **64** (2001) 113107.
- [28] C. Mudry, P.W. Brouwer and A. Furusaki, *Phys. Rev. B* **62** (2000) 8249; G. Chiappe, E. Louis, M.J. Sanchez and J.A. Verges, *Phys. Rev. B* **69** (2004) 201405.
- [29] J. Kiskis and R. Narayanan, *Phys. Rev. D* **64** (2001) 117502.
- [30] K.A. Muttalib, Y. Chen, M.E.H. Ismail and V.N. Nicopoulos, *Phys. Rev. Lett.* **71** (1993) 471; Y. Chen and K.A. Muttalib, *J. Phys.:Condens. Matter* **6** (1994) L293.
- [31] A.M. Garcia-Garcia and J.J.M. Verbaarschot, *Phys. Rev. E* **67** (2003) 046104.
- [32] A.M. Garcia-Garcia and K. Takahashi, *Nucl.Phys.* **B700** (2004) 361.
- [33] V.E. Kravtsov and A.M. Tselik, *Phys. Rev. B* **68** (2000) 9888.
- [34] B. Sutherland, *J. Math. Phys.* **12** (1971) 246; F. Calogero, *J. Math. Phys.* **10** (1969) 2191.
- [35] P.H. Damgaard, U.M. Heller, R. Niclasen and K. Rummukainen, *Nucl.Phys.* **B583** (2000) 347.
- [36] T. Schaefer and E.V. Shuryak, *Phys. Rev. D* **53** (1996) 6522.
- [37] A.M. Garcia-Garcia and J.C. Osborn, in preparation.
- [38] M. Golterman and Y. Shamir, *Phys. Rev. D* **68** (2003) 074501; *Phys. Rev. D* **71** (2005) 071502; *Phys. Rev. D* **72** (2005) 034501.
- [39] I. Horvath, N. Isgur, J. McCune and H.B. Thacker, *Phys. Rev. D* **65** (2002) 014502; I. Horvath, et. al., *Phys. Rev. D* **66** (2002) 034501; I. Horvath, *Nucl. Phys.* **B710** (2005) 464; Erratum-ibid. **B714** (2005) 175; I. Horvath, et.al., *Phys. Lett.* **B612** (2005) 21; A. Alexandru, I. Horvath and J.B. Zhang, *Phys. Rev. D* **72** (2005) 034506; V. Weinberg, E.-M. Ilgenfritz, K. Koller, Y. Koma, G. Schierholz and T. Streuer, *PoS LAT2005* (2005) 171; C. Bernard, et.al., *PoS LAT2005* (2005) 299.